Metals **2012**, *2*, 329-343; doi:10.3390/met2030329

OPEN ACCESS

metals

ISSN 2075-4701
www.mdpi.com/journal/metals/

Review

Application of Severe Plastic Deformation Techniques to Magnesium for Enhanced Hydrogen Sorption Properties

Jacques Huot [1,*], Nataliya Ye. Skryabina [2] and Daniel Fruchart [3]

[1] Physics Department, Université du Québec à Trois-Rivières, 3351 des Forges, Trois-Rivières, Québec, G9A 5H7, Canada

[2] Department of Physics, Perm State University, 15, Bukirev street, 614990, Perm, Russia; E-Mail: natskryabina@mail.ru

[3] Institut Néel, 25 rue des Martyrs, BP 166, 38042 Grenoble Cedex 9, France; E-Mail: daniel.fruchart@grenoble.cnrs.fr

* Author to whom correspondence should be addressed; E-Mail: jacques.huot@uqtr.ca; Tel.: +1-819-376-5011 (ext. 3576); Fax: +1-819-376-5164.

Received: 1 June 2012; in revised form: 14 August 2012 / Accepted: 15 August 2012 / Published: 31 August 2012

Abstract: In this paper we review the latest developments in the use of severe plastic deformation (SPD) techniques for enhancement of hydrogen sorption properties of magnesium and magnesium alloys. Main focus will be on two techniques: Equal Channel Angular Pressing (ECAP) and Cold Rolling (CR). After a brief description of these two techniques we will discuss their effects on the texture and hydrogen sorption properties of magnesium alloys. In particular, the effect of the processing temperature in ECAP on texture will be demonstrated. We also show that ECAP and CR have produced different textures. Despite the scarcity of experimental results, the investigations up to now indicate that SPD techniques produce metal hydrides with enhanced hydrogen storage properties.

Keywords: magnesium; magnesium alloys; severe plastic deformations; ECAP; Cold Rolling

---

1. Introduction

Since the last few years the effects of mechanical deformation on the hydrogen storage behavior of metal hydrides have been intensively studied. Mechanochemistry, mainly performed using Ball

Milling (BM), has demonstrated the possibility to conduct various reactions, such as synthesis of nanocrystalline and amorphous materials at low temperatures without dissolution or fusion of the reactants. Forty years after the pioneering works of Benjamin [1] the mechanochemical treatment of substances in producing new thermodynamically stable and metastable materials, often non-achievable by traditional methods, is well established and received industrial applications. While the method is progressing at the industrial level, knowledge about the physical mechanisms operating during the mechanochemical treatment (e.g., ball milling) is still very limited due to serious difficulties in quantifying this complex process [2].

The mechanochemical techniques of ball-milling (BM) and severe plastic deformation (SPD) methods are widely used in research laboratories as well as in the industry. In the field of metal hydrides BM is intensively used for preparation of new compounds and to obtain nanocrystalline structure. Mechanical milling effects could be enhanced by changing parameters such as milling atmosphere (reactive milling), temperature, addition of anti-sticking agents, *etc.* This level of sophistication led to impressive results in enhancement of hydrogen storage properties of metal hydrides by the use of mechanical milling. The next challenge is to scale-up these types of technologies to industrial levels. Here the main hurdle may be the high energy milling (power and time) which is most usually needed for improving metal hydride properties. This imposes additional requirements in terms of specific energy of the milling machine and size of batches that could be processed. These problems are compounded if the milling has to be performed under hydrogen pressure and at high temperature. One also has to take into account the safety aspect of handling metal hydrides. The engineering aspects of these problems could surely be solved. The main challenge will be to keep the capital and operation cost low in order to make the technology competitive. However, the use of this technique poses the problem of scaling-up a high-energy density method.

In the case of SPD it has just recently been used for metal hydrides and the results are relatively scarce. In an early investigation, Ueda *et al.* have prepared a Mg–Ni laminated composite by cold rolling stacked Mg and Ni sheets [3]. However, to obtain the intermetallic Mg_2Ni the samples had to be heat treated at 673 K. Similar results were later found by Pedneault *et al*. [4,5]. They showed that cold rolling combined with heat treatment resulted in nanostructured metal hydrides with good electrochemical properties. In the case of Ti-based alloys, Zhang *et al*. [5,6] studied the effect of cold rolling on the hydrogen sorption properties of Ti–22Al–27Nb alloy and found better hydrogenation kinetics for cold rolled samples but only for the first hydrogenation cycle. Magnesium alloys have been studied by a few groups using different SPD techniques or combination of them [6–23]. These studies will be discussed in more details in the next sections but the general conclusion is that SPD techniques could improve the hydrogen sorption properties of magnesium alloys.

One important advantage of SPD techniques over high energy milling is that they are potentially easier to scale up to industrial level. Therefore, the study of SPD applied to metal hydrides is interesting from a fundamental point of view because of the different action of SPD on the processed material compared to high energy milling and also from a practical point of view because of the possibility of reducing cost of hydrides processing. In this paper we will review the use of two SPD techniques, Equal Channel Angular Pressing (ECAP) and Cold Rolling (CR) for the preparation of magnesium for hydrogen storage. After a short description of each technique we will present recent studies of the use of them in the case of magnesium. More specific techniques such as High Pressure

Torsion (HPT) and Fast Forging (FF) are not considered here because at this moment very few investigations have been realized.

2. Equal Channel Angular Pressing

2.1. Description of the Technique

In the Equal Channel Angular Pressing (ECAP) severe plastic deformations are introduced into a material by forcing a sample (billet) with a piston through a die consisting of two channels of equal cross-section, which intersect at an angle (Φ) between 90° and 120° [24] (see Figure 1). The outer arc of curvature where the two channels intersect is labeled Ψ. Since the billet assumes the form and the cross-section of the die, it can be repeatedly processed to increase the microstrain density and simultaneously reduce the size of crystallites to meso- or nanometer down to 40 to 100 nm range. ECAP is quite efficient in processing metals and allows to produce porosity-free materials in substantial quantities with lower concentration of impurities and at a lower cost than ball-milling [25]. Through the crystallite size refinement process, the proportion of high angle grain boundary (HAGB) increases due to dislocations recovery [26]. High texturation effects could also be introduced by this process, thus organizing specific grain boundaries distributions, indeed depending on the crystal symmetry of the processed system (e.g., cubic *versus* hexagonal).

Figure 1. Schematic illustration of Equal Channel Angular Pressing (ECAP).

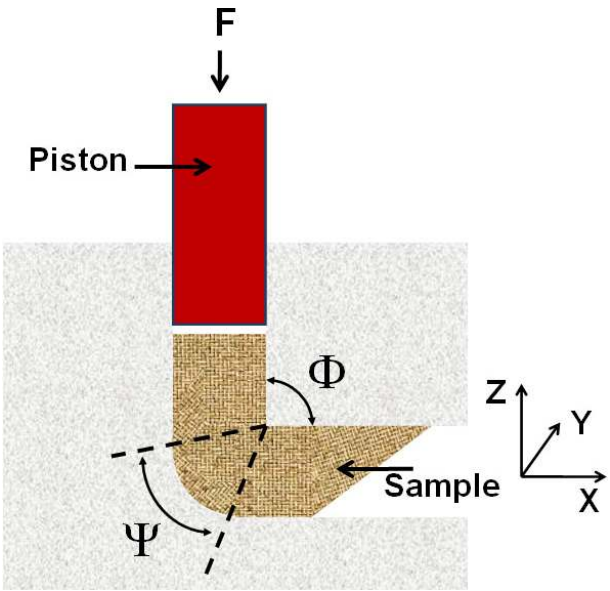

2.2. Strain

The equivalent strain (ε) introduced in the material by the ECAP process is determined by an equation incorporating the angle between the two parts of the channel, Φ, and the angle representing the outer arc of curvature where the two parts of the channel intersect, Ψ. The relationship given by:

$$\varepsilon = \frac{2\,N}{\sqrt{3}}\left[\cot\left\{\left(\frac{\Phi}{2}\right)+\left(\frac{\Psi}{2}\right)\right\}\right] + \Psi\, f\{N, \Phi, \Psi\} \quad (1)$$

where N is the number of passes through the die [27], and accounting the weakness of the f term contribution an expression that is often simplified [7], to:

$$\varepsilon = 1.15\, N \cot\left(\frac{\Phi}{2}\right) \tag{2}$$

However, if the number of passes seems to be a dominant parameter, the most important refinement of the microstructure takes place during the first pressing passes, since the development of an ultrafine grain size leads to an increase of the yield stress.

2.3. Effect of Billet Rotation

From Figure 1 it could be seen that after a single pressing a cubic element is sheared into a rhombohedral shape. If the same billet is pressed a second time then the operator has the choice to insert the billet with or without rotation. It has been recognized that, for repetitive pressing, the overall shearing characteristics within the crystalline sample may be changed by a rotation of the sample between the individual pressings [28]. When samples are pressed repetitively, different slip systems may be introduced by rotating the samples about the X-axis between consecutive passes through the die. Several processing routes have been identified for use in ECAP: route A in which the sample is pressed repetitively without rotation, route B_C in which the sample is rotated by 90° in the same sense between each pass and route C where the sample is rotated by 180° between passes [29]. More complex combination of these routes could also be performed.

Inspection of Figure 2 shows that route A markedly increase the distortion of the rhombohedron, route B increases the distortion in the X and Z planes and route C restores the cubic element so that strain has been introduced but with no ultimate distortion of the bulk of the sample [30]. We are looking for a route that will introduce maximum strain in all directions while recovering a cubic shape after N passes. Immediately, we see that route A is not optimal because the cubic structure is not recovered. In route C the cubic structure is recovered after each $2N$ pressings but no deformation is induced in the Z plane. Therefore, the only optimal route is B_C since introducing strains in each plane while recovering a cubic structure after $4N$ passes.

Figure 2. Characteristics of most important processing routes: (**A**) The modes of successive passes in the ECAP die; (**B**) Effective deformation of the shape of a billet.

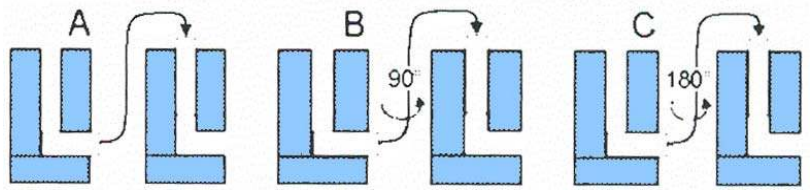

(A)

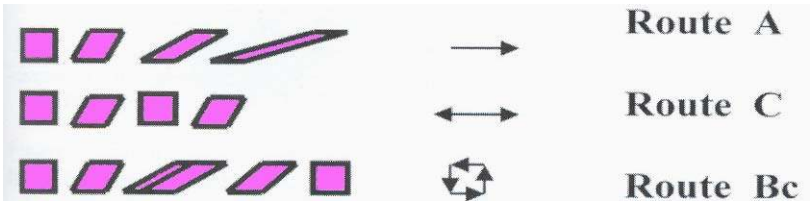

(B)

It has been shown experimentally that, when using an ECAP die with an angle of 90° between the two parts of the channel, optimum processing is achieved using route B_C because this leads most rapidly both to an array of reasonably equiaxed grains and to a high fraction of grain boundaries having high angles of misorientation [31]. The influence of various ECAP parameters such as value of angles Ψ and Φ, pressing speed, temperature, and back pressure are discussed in a recent review [24].

2.4. ECAP Effect on Magnesium

The effect of ECAP on the hydrogen storage behavior of Mg-based alloys has been investigated by Skripnyuk *et al.* [6–9]. The structural alloy ZK60 of composition Mg–4.95 wt % Zn–0.71 wt % Zr were processed by high energy ball milling (HEBM), ECAP, and a combination of ECAP and HEBM. The ECAP processing was made through route A with eight passes at 250–300 °C and one additional pass at room temperature [6]. The results show that after ECAP/HEBM treatment the hysteresis in the pressure-composition isotherm completely disappears. However, the most important effect of processing was on the hydrogen desorption kinetics. As shown in Figure 3, ECAP processed samples shows much improved kinetics compare to as-cast and annealed samples. The fact that ZK60 desorbed hydrogen faster than HEBM-processed Mg was supposed being due to the catalytic effect of Zn and Zr. In turn, ECAP, HEBM, and ECAP/HEBM-processed alloys desorbed hydrogen at approximately the same rate, which was much higher than the desorption rate for annealed ZK60. Also combined ECAP/HEBM treatment did not improved the kinetics of desorption as compared to the effect of ECAP alone.

Figure 3. Kinetics of hydrogen desorption at 300 °C from differently processed samples of ZK60 alloy and from high energy ball milling (HEBM)-processed pure Mg. [6]

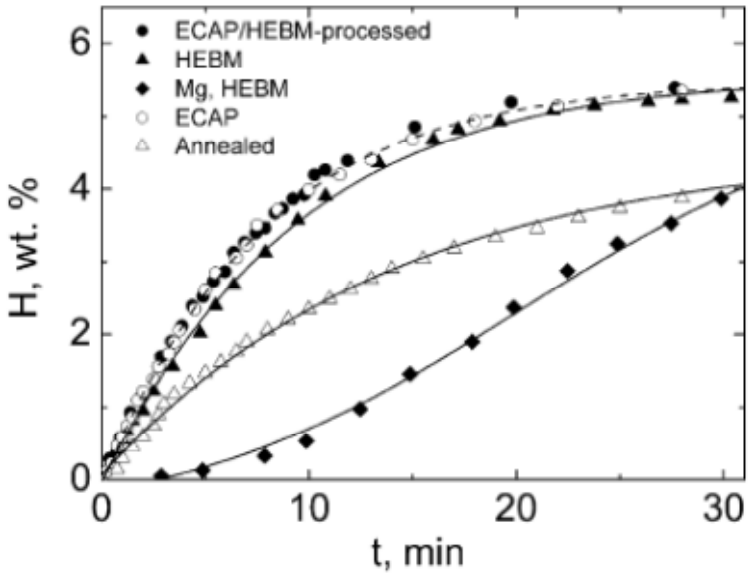

In the case of as-cast eutectic Mg-Ni alloy, after 10 ECAP passes (route B_C) sub-micrometer size of Mg and Mg_2Ni grains was achieved [7]. The Mg grains showed supersaturation in Ni, which was non-homogeneously distributed across the grains. The Ni concentrations in the Mg grains with high dislocation density were consistently higher than in the grains with fewer dislocations. Gravimetric

hydrogen storage capacity of about 6 wt % was measured. Pressure-composition isotherm measurements indicated that both Mg and Mg_2Ni phases are destabilized compare to their as-cast counterparts. The ECAP processed alloy also exhibited excellent hydrogen desorption kinetics. In fact, in terms of hydrogen desorption pressure the ECAP treated Mg-Ni alloy outperformed the alloys of similar composition nanostructured by alternative processing techniques [7].

Recently, Skripnyuk *et al*. investigated the hydrogenation properties of magnesium doped with carbon nano-tubes (CNT). When HEBM is used to synthesize Mg-CNT mixtures destruction of CNT is happening after a relatively short time of milling. Their idea was to use ECAP to get a good contact between Mg and CNT [9]. They found that ECAP led to a slower absorption/desorption kinetics at the initial stages of the processes, and to their acceleration at the later stages. Two competing factors are proposed to explain the complex effect of ECAP on the hydrogenation kinetics of the composite. Namely, a decrease in hydrogen diffusivity along the CNTs due to their rupture and kinking, and concurrent enhancement of the hydrogen diffusion kinetics in the Mg matrix [9].

In another investigation, Løcken *et al.* used ECAP and HEBM to process the ternary eutectic $Mg–Mg_2Ni–MmMg_{12}$ (72 wt % Mg–20 wt % Ni–8 wt % Mm, Mm = mischmetal) [32]. After eight ECAP passes at 400 °C (route B_C) an improvement in the hydrogen absorption and desorption rates was noticed. However, HEBM gave an even larger improvement and reduced the absorption and desorption times to one third of those of the as-cast alloy.

2.5. Effect of Extrusion Temperature

In more recent works, the processing temperature as was studied a key parameter for grain size control [11,33,34]. Figure 4 shows the effect of ECAP temperature processing for AZ31 alloy. This figure shows the effect of two ECAP passes (mode B_C) performed at different temperatures. Each experiment was performed by starting from the as-cast material. With increasing the number of passes the elongations of fractures is increasing, mainly for temperatures lower than 200 °C. For higher temperature (e.g., 250 °C) the yield stress (or the maximum stress) shows only small changes. The as-cast structure, shown in Figure 4A, contains large well crystallized grains (from 10 to 50 μm). Figure 4B shows that after two ECAP passes at 150 °C, the initial structure is severely crushed by the deformation process. Grains are elongated and have a general orientation. A similar structure is still seen after two passes at 200 °C as presented in Figure 4C. A completely different structure is obtained by ECAP at 250 °C as displayed in Figure 4D. Here, there are no signs of deformation. This indicates that recrystallization took place during ECAP deformation. If the processing temperature is increased to 300 °C, after two ECAP passes the sample is fully recrystallized. There are no remains of plastic deformation effect but during ECAP there was a grain size growth. These results clearly show that dynamic re-crystallization could occur during ECAP and that the operation temperature can markedly influence the microstructure of the sample, thus the hydrogenation/dehydrogenation reactions. Practically, during the SPD process a few ten degrees increase of temperature may occurs for some systems.

Comparative experiments performed more recently on ECAP processed AZ31 samples reveal that the most effective reaction in terms of hydrogen absorption/desorption kinetics correspond to samples treated in the range of brittle to ductile mechanical characteristics (150–210 °C—see Figure 4B,C).

Figure 4. Optical micrographs of AZ31 magnesium alloy. (**A**) as-cast; (**B**) two passes at 150 °C; (**C**) two passes at 200 °C; (**D**) two passes at 250 °C; (**E**) two passes at 300 °C.

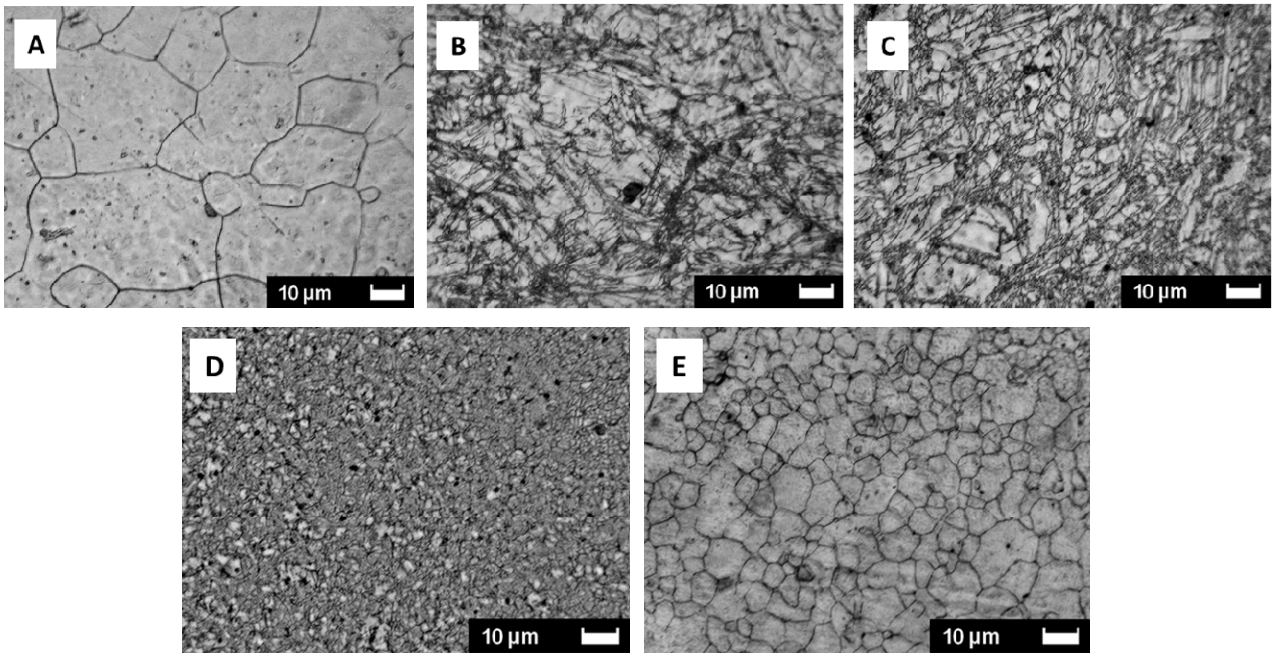

Figure 5 shows the evolution of texture for AZ31 magnesium alloy for different ECAP routes. It is seen that a very marked texture is delivered by route A processing, contrarily to mode B_C that distributes almost equally the grains along all crystalline directions. Also, the profiles of lines are much broadened for the route B_C than for route A, meaning that more defects are developed during the multi-orientation process B_C. So, as said above, both effects impact quite differently the hydrogen sorption properties.

Figure 5. Texture of AZ31 magnesium alloy. (**A**) One pass at RT, mode A; (**B**) Six passes at RT, mode B_C. Orientations are color coded. (002)-blue; (100)-red; (101)-black; (110)-green.

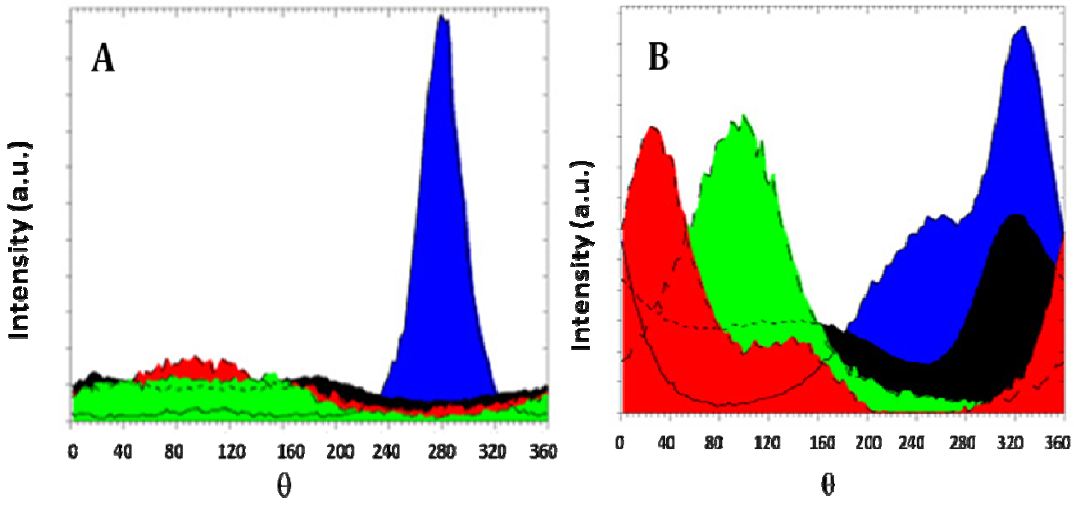

Samples processed N-times following route A ($2 < N < 8$) develop an initial incubation time before a continuous hydrogen absorption rate, while absorption started readily in samples processed by route B_C. It may be concluded that the shape, the size and the texture (as shown on Figure 5) of the deformed

grains are pertinent parameters to be consider in the hydrogen activation and diffusion processes [18]. For these samples, an hydrogen uptake up to ~7.6% was measured.

3. Cold Rolling

3.1. Description of the Technique

In cold rolling technique (CR), a sheet of metal is introduced between rollers where it is compressed and squeezed (Figure 6). The hardness and other properties of the finished product depends on the amount of strain induced in each Cr pass.

Figure 6. Schematic illustration of Cold Rolling (CR).

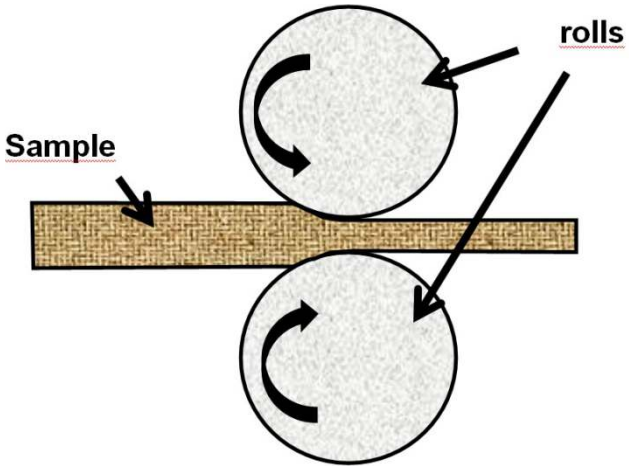

Usually, rolling is classified according to the processing temperature as compared with the metal re-crystallization temperature. In Hot Rolling (HR) the process is carried out at a temperature exceeding the re-crystallization temperature of the rolled material while in Cold Rolling (CR) rolling temperature is below re-crystallization temperature. In this review only CR will be discussed.

3.2. Strain

If we represent the rolling direction (RD), transverse direction (TD) and normal direction (ND) by directions by subscript 1, 2, and 3 respectively then, to a very rough approximation for macroscopic sheets, rolling deformation is plane strain compression for which $\varepsilon_{11} = -\varepsilon_{33}$ and all other strains $\varepsilon_{22} = \varepsilon_{12} = \varepsilon_{13} = \varepsilon_{23} = 0$. Under these idealized assumptions the effective strain equals the von Mises equivalent strain [35].

$$\varepsilon = \sqrt{\frac{2\,(\varepsilon_{11}^2 + \varepsilon_{22}^2 + \varepsilon_{33}^2 + 2\varepsilon_{12}^2 + 2\varepsilon_{13}^2 + 2\varepsilon_{23}^2)}{3}} = \sqrt{\frac{2}{3}}\,\varepsilon_{11} \tag{3}$$

In this idealized situation the strain is in normal direction contrary to HPT and ECAP processes which produce mainly shear deformations. However, in real situation deformation in the rolled sheet is strongly affected by frictional condition between the rolls and the metals. It is well-known that under high friction conditions the metals deform inhomogeneously through thickness because a large amount of redundant shear strain is introduced in the surface regions [36].

3.3. Accumulative Roll Bonding

In accumulative roll bonding (ARB) [37] the starting sample is made of a stack of two or more thin foils. The foils' interfaces could be surface-treated in order to enhance bond strength. The foils could be made of the same element or of different elements in the desired stoichiometric composition. The stack is then rolled as in as in a conventional roll- bonding process. Then, the length of rolled material is sectioned into two halves. The sectioned foils are stacked one on top of the other and rolled again. The whole process is repeated for the desired number of times. In effect, ARB rolling is not only a deformation method but also a bonding process. The process can introduce ultra-high plastic strain without any geometrical change.

It should be noted, that in ARB process half of the surface regions comes to the center in the next cycle. This results in complicated distributions of the surface regions with large shear strain through thickness of the foil. With a 50% thickness reduction at each rolling pass and assuming no lateral spreading of the material (von Mises yield criterion and plane strain condition) the equivalent plastic strain after N cycles is [37]:

$$\varepsilon = \frac{2n}{\sqrt{3}} \ln(1/2) \cong 0.8\,N \tag{4}$$

From this expression we see that as the ARB procedure could be applied for a limitless number of time, large plastic strain could be reached for even a few numbers of rolls [38].

3.4. Cold rolling of Magnesium

Magnesium has a limited number of slip planes and work hardening occurs rapidly. Thus, after only a few rolling passes, a magnesium foil will quickly break up in small pieces. Therefore, rolling many times (more than 10 rolling passes) could be difficult. However, for hydrogen storage applications and mechanical integrity is not so important. In fact, after a few hydrogenations many metal hydrides turn into powder because of the important decrepitation due to the significant volume change during hydrogenation. Consequently, work hardening is not a significant problem for hydrogen storage applications.

To our knowledge, Ueda *et al.* were the first to try to synthesize a metal hydride (Mg_2Ni) using cold rolling of raw elements followed by heat treatment [3]. When using the stoichiometry 2Mg + Ni, single phase Mg_2Ni was obtained, and the sample could be completely hydrogenated to Mg_2NiH_4. Interdiffusion between Mg and Ni during heat treatment was the mechanism for the formation of Mg_2Ni [3]. Mg-Ni system for electrochemical applications was also studied by Pednault *et al.* [4,5]. They investigated the structural and electrochemical evolution of 2Mg–Ni cold-rolled samples as a function of the number of rolling passes as well as heat treatment. They found that nanocrystalline Mg_2Ni alloy was obtained by an appropriate three step process involving rolling, heat treatment and rolling again. The best results were obtained by first rolling 90 times, followed by a heat treatment at 400 °C for 4 h and roll again 20 times. The treated material displayed an initial discharge capacity of 205 $mAhg^{-1}$,which is quite similar to that obtained with ball-milled Mg_2Ni alloy [4].

For Mg-Pd system, Dufour and Huot have shown that cold rolled samples have a much better air contamination resistance than the same material prepared by ball milling [23].Takeichi *et al.* [39] as

well as Dufour and Huot [22] have also shown that the alloy Mg_6Pd could be synthesized by cold rolling followed by heat treatment. Other Mg-X systems such as Mg-Ti [21,40], Mg-Al [41], Mg-Cu [39,42], Mg-Fe [11,13] as well as commercial Mg-Zr-Zn alloy [43] have been investigated.

3.5. Texture Evolution of Cold Rolled Alloys

Figure 7 shows the evolution of texture in cold rolled magnesium. Rolling was performed at room temperature and there was a 50% thickness reduction at each pass. From Figure 7A we see that after just one rolling pass the material is already highly textured. Further increase of the number of deformation passes leads to insignificant decrease in the intensity of the texture maximum ((002) direction). It should be noted that the width of maximum remains relatively broad in all cases. This means that the deformation is spread over the sample. In the case of ECAP the deformation is not so spread as for CR since the latter changes strongly the overall dimensions of the sample. In our opinion, it is due to the fact that in the course of rolling deformation of a sample is carried out both as a compression, and a shift of deformation. Therefore the structure comes out with larger dispersion than in the case of ECAP.

Figure 7. Pole figure of cold rolled magnesium. Orientations are color coded. (002)-blue; (100)-red; (101)-black. (**A**): 1 rolling pass; (**B**): 10 rolling passes; (**C**): 100 rolling passes.

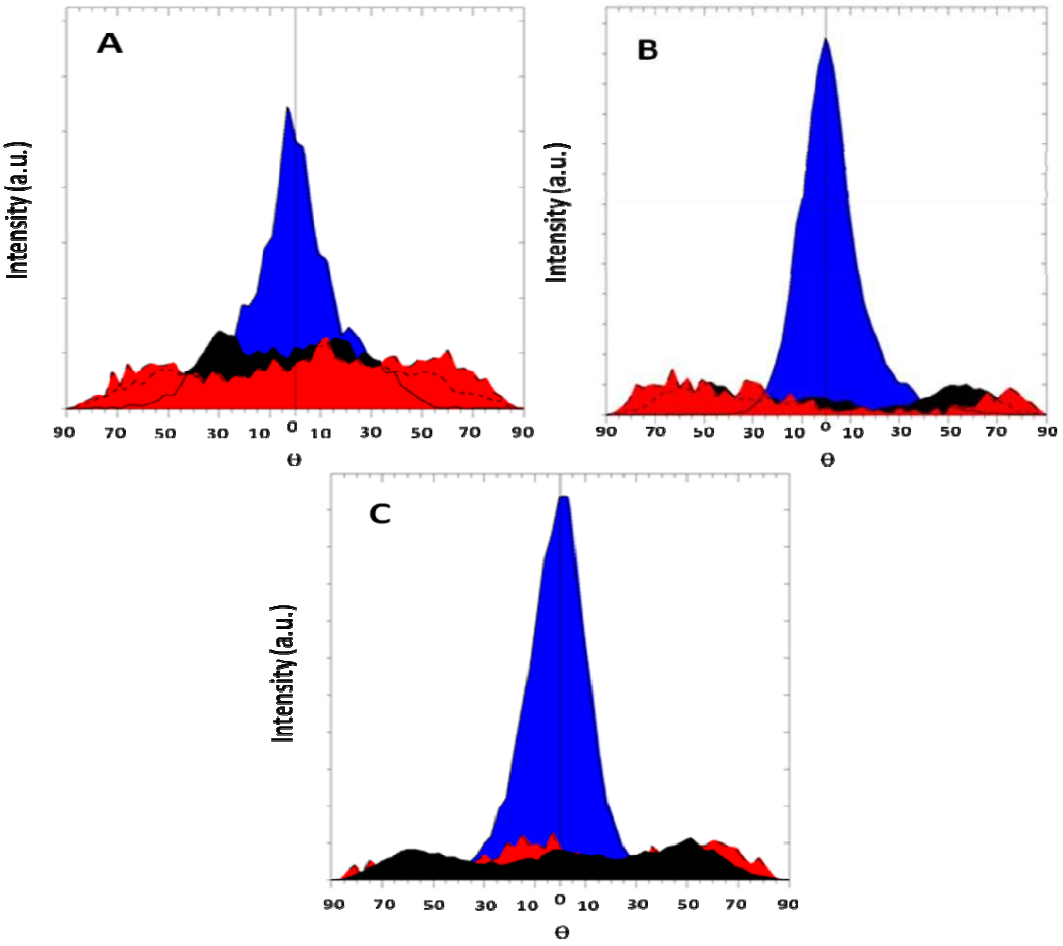

3.6. Hydrogen Sorption Properties of Cold Rolled Magnesium Alloys

Most of the studies of SPD on magnesium alloys have used ECAP techniques: to our knowledge the only systematic investigation of effect of cold rolling on commercial magnesium alloys have been reported by Amira and Huot on four different as-cast and die-cast alloys (AZ91, MRI153, AXJ530 and ZAEX10430) [18]. Here we report the main features of AZ91D alloy compared to pure magnesium. Plates of AZ91D and pure magnesium were first rolled 50 times in air. A 50% reduction at each roll was obtained by folding the plates in two between two successive rolls. Final thickness was about 0.3 mm. In order to introduce nucleation points for the hydride phase, after the final roll the material was mixed with 5 wt % of MgH_2 and ball milled for 30 minutes. Hydrogenation was performed at 623 K under hydrogen pressure of 2 MPa for the absorption and 0.01 MPa for desorption. Figure 8 compares the first hydrogenation (activation) of cold rolled AZ91D and magnesium.

Figure 8. First hydrogenation (activation) of cold rolled AZ91D and magnesium.

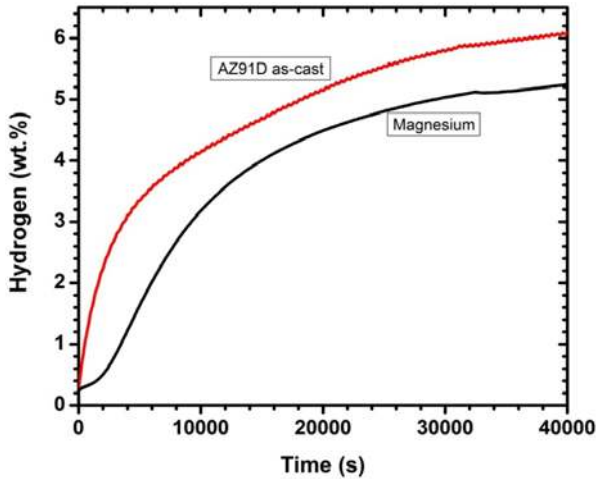

The first hydrogenations of unrolled materials are not shown because they are too slow, effectively taking a few days for partial activation. From Figure 8 one can see that AZ91D activate faster than pure magnesium but the main difference is not so much the intrinsic kinetic but the fact that the alloy do not have the incubation time shown by pure magnesium. The absence of incubation time is not fully understood but it may be due to the presence of precipitates of $Mg_{17}Al_{12}$ and Al_8Mn_5 compounds seen in the micrograph presented on Figure 9.

Figure 9. Microstructure of as-cast AZ91D. Primary α-Mg with discontinuous and divorced $Mg_{17}Al_{12}$ eutectic. The white particles are Al_8Mn_5 compound (γ-brass).

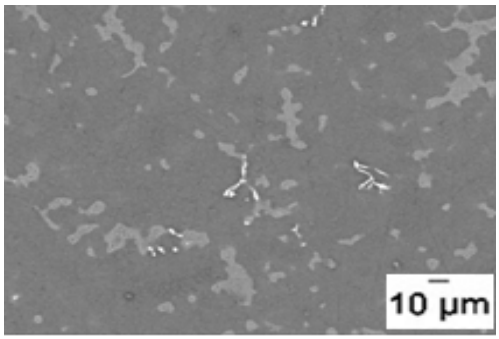

Dehydrogenation of kinetics of cold rolled AZ91D and magnesium are shown in Figure 10. The alloy has faster dehydrogenation kinetics and the incubation time is shorter than pure magnesium. In subsequent cycle, the AZ91D alloys kept its faster sorption kinetics compared to pure magnesium [18].

Figure 10. Dehydrogenation kinetics of cold rolled AZ91D and magnesium.

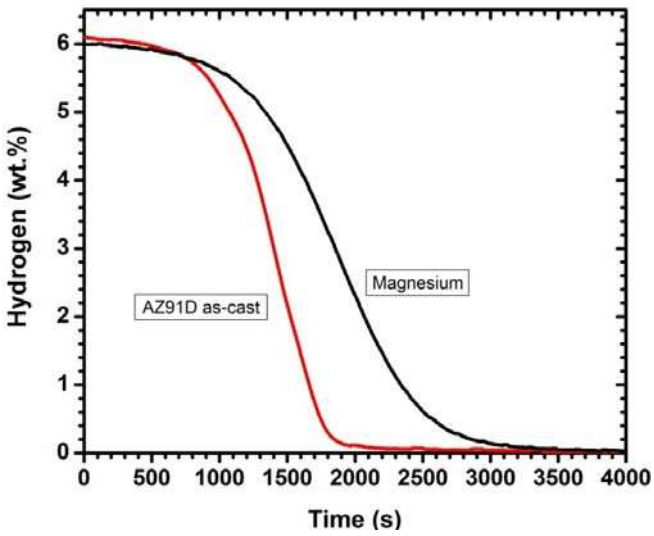

4. Conclusions

Mechanical milling and severe plastic deformation are valuable methods for the synthesis and preparation of metal hydrides, but the former is presently much more used than the later. Up to now, for SPD technique the level of understanding the impact of these techniques on the hydrogen storage properties of metal hydrides is still relatively small. Only a limited number of papers have been published and just a few research groups are investigating metal hydrides applications of SPD. However, first results are encouraging and show similarities with mechanical milling in the effectiveness of obtaining a nanocrystalline structure and enhancement of hydrogen storage properties. Some SPD techniques such as HPT could face the same and maybe bigger scaling-up problems but others, for instance, Cold Rolling, Fast Forging and even ECAP could be more easily adopted by the industry. The capital and operating cost of these techniques is potentially much less than mechanical milling. For example, a recent investigation has shown that at laboratory scale cold rolling could produce similar enhancement of hydrogen storage properties of magnesium hydride than ball milling but with energy requirement and processing time reduced by an order of magnitude [20]. The same reduction is expected at industrial level.

Because of the multiple parameters of ECAP (angle of channel, type of routes, number of passes, rate of process, temperature of sample, *etc.*) this technique offers a large panel of control factors to design the microstructure, the texture as well as the defect density (from dislocations to twins) to apply to the wide mechanical strength properties of commercially available magnesium alloys. Cold rolling may not be as sophisticated as ECAP in making materials with a wide range of textures but its potential for industrial applications may be higher.

From a more fundamental point of view, both mechanical milling and SPD could produce materials with new characteristics such as nanocrystalline structure, metastable phases, high density of defects,

texture, important microstrain, *etc.* Each of these features could have an impact on the hydrogen storage behavior but the exact multiple mechanisms are usually not fully understood. More studies on the basic mechanism of mechanical effect through milling and SPD within the scope of hydrogen storage are needed.

Acknowledgments

The authors would like to thanks the Ministry of Education of Perm Region (Russia) for funding project C-26/211. Jacques Huot would like to thanks the Natural Science and Engineering Council of Canada and the Research Council of Norway for additional funding that permitted a sabbatical leave at the Institute for Energy Technology (IFE) in Norway.

References

1. Benjamin, J.S. Mechanical alloying. *Sci. Am.* **1976**, *235*, 40–49.
2. Suryanarayana, C. Recent developments in mechanical alloying. *Rev. Adv. Mater. Sci.* **2008**, *18*, 203–211.
3. Ueda, T.T.; Tsukahara, M.; Kamiya, Y.; Kikuchi, S. Preparation and hydrogen storage properties of Mg-Ni-Mg_2Ni laminate composites. *J. Alloy. Compd.* **2004**, *386*, 253–257.
4. Pedneault, S.; Huot, J.; Roué, L. Nanostructured Mg_2Ni materials prepared by cold rolling and used as negative electrode for Ni-MH batteries. *J. Power Source.* **2008**, *185*, 566–569.
5. Pedneault, S.; Roué, L.; Huot, J. Synthesis of metal hydrides by cold rolling. *Mater. Sci. Forum* **2008**, *570*, 33–38.
6. Skripnyuk, V.; Rabkin, E.; Estrin, Y.; Lapovok, R. The effect of ball milling and equal channel angular pressing on hydrogen absorption/desorption properties of Mg-4.95 wt % Zn-0.71wt %Zr (ZK60) alloy. *Acta Mater.* **2004**, *52*, 405–414.
7. Skripnyuk, V.; Buchman, E.; Rabkin, E.; Estrin, Y.; Popov, M.; Jorgensen, S. The effect of equal channel angular pressing on hydrogen storage properties of a eutectic Mg-Ni alloy. *J. Alloy. Compd.* **2007**, *436*, 99–106.
8. Skripnyuk, V.M.; Rabkin, E.; Estrin, Y.; Lapovok, R. Improving hydrogen storage properties of magnesium based alloys by equal channel angular pressing. *Int. J. Hydrog. Energy* **2009**, *34*, 6320–6324.
9. Skripnyuk, V.M.; Rabkin, E.; Bendersky, L.A.; Magrez, A.; Carreño-Morelli, E.; Estrin, Y. Hydrogen storage properties of as-synthesized and severely deformed magnesium-multiwall carbon nanotubes composite. *Int. J. Hydrog. Energy* **2010**, *35*, 5471–5478.
10. Leiva, D.R.; Floriano, R.; Huot, J.; Jorge, A.M.; Bolfarini, C.; Kiminami, C.S.; Ishikawa, T.T.; Botta, W.J. Nanostructured MgH_2 prepared by cold rolling and cold forging. *J. Alloy. Compd.* **2011**, *509*, S444–S448.
11. Leiva, D.R.; Fruchart, D.; Bacia, M.; Girard, G.; Skryabina, N.; Villela, A.C.S.; Miraglia, S.; Santos, D.S.; Botta, W.J. Mg alloy for hydrogen storage processed by SPD. *Int. J. Mater. Res.* **2009**, *100*, 1739–1746.

12. Leiva, D.R.; Huot, J.; Ishikawa, T.T.; Bolfarini, C.; Kiminami, C.S.; Jorge, A.M.; Botta, W.J. Hydrogen activation behavior of commercial magnesium processed by different severe plastic deformation routes. *Mater. Sci. Forum* **2011**, *667–669*, 1047–1051.
13. Leiva, D.R.; Jorge, A.M.; Ishikawa, T.T.; Huot, J.; Fruchart, D.; Miraglia, S.; Kiminami, C.S.; Botta, W.J. Nanoscale grain refinement and H-sorption properties of MgH_2 processed by high-pressure torsion and other mechanical routes. *Adv. Eng. Mater.* **2010**, *112*, 786–792.
14. Lima, G.F.; Jorge, A.M.; Leiva, D.R.; Kiminami, C.S.; Bolfarini, C.; Botta, W.J. Severe plastic deformation of Mg-Fe powders to produce bulk hydrides. *J. Phys. Conf. Ser.* **2009**, *144*, doi:10.1088/1742-6596/144/1/012015.
15. Krystian, M.; Zehetbauer, M.J.; Kropik, H.; Mingler, B.; Krexner, G. Hydrogen storage properties of bulk nanostructured ZK60 Mg alloy processed by equal channel angular pressing. *J. Alloy. Compd.* **2011**, *509*, S449–S455.
16. Vincent, S.D.; Lang, J.; Huot, J. Addition of catalysts to magnesium hydride by means of cold rolling. *J. Alloy. Compd.* **2012**, *512*, 290–295.
17. Bellemare, J.; Huot, J. Hydrogen storage properties of cold rolled magnesium hydrides with oxides catalysts. *J. Alloy. Compd.* **2012**, *512*, 33–38.
18. Amira, S.; Huot, J. Effect of cold rolling on hydrogen sorption properties of die-cast and as-cast magnesium alloys. *J. Alloy. Comd.* **2012**, *520*, 287–294.
19. Vincent, S.D.; Huot, J. Effect of air contamination on ball milling and cold rolling of magnesium hydride. *J. Alloy. Compd.* **2011**, *509*, L175–L179.
20. Lang, J.; Huot, J. A new approach to the processing of metal hydrides. *J. Alloy. Compd.* **2011**, *509*, L18–L22.
21. Danaie, M.; Mauer, C.; Mitlin, D.; Huot, J. Hydrogen storage in bulk Mg-Ti and Mg-stainless steel multilayer composites synthesized via accumulative roll-bonding (ARB). *Int. J. Hydrog. Energy* **2011**, *36*, 3022–3036.
22. Dufour, J.; Huot, J. Study of Mg_6Pd alloy synthesized by cold rolling. *J. Alloy. Compd.* **2007**, *446–447*, 147–151.
23. Dufour, J.; Huot, J. Rapid activation, enhanced hydrogen sorption kinetics and air resistance in laminated Mg–Pd 2.5 at. %. *J. Alloy. Compod.* **2007**, *439*, L5–L7.
24. Valiev, R.; Langdon, T.G. Principles of equal-channel angular pressing as a processing tool for grain refinement. *Prog. Mater. Sci.* **2006**, *51*, 881–981.
25. Langdon, T.G. The characteristic of grain refinement in materials processed by severe plastic deformation. *Rev. Adv. Mater. Sci.* **2006**, *13*, 6–14.
26. Huang, C.X.; Yang, H.J.; Wu, S.D.; Zhang, Z.F. Microstructural characterizations of Cu processed by ECAP from 4 to 24 passes. *Mater. Sci. Forum* **2008**, *584–586*, 333–337.
27. Iwahashi, Y.; Wang, J.; Horita, Z.; Nemoto, M.; Langdon, T.G. Principle of equal-channel angular pressing for the processing of ultra-fine grained materials. *Scr. Mater.* **1996**, *35*, 143–146.
28. Furukawa, M.; Horita, Z.; Nemoto, M.; Langdon, T.G. Review: Processing of metals by equal-channel angular pressing. *J. Mater. Sci.* **2001**, *36*, 2835–2843.
29. Langdon, T.G. The principles of grain refinement in equal-channel angular pressing. *Mater. Sci. Eng. A* **2007**, *462*, 3–11.

30. Furukawa, M.; Iwahashi, Y.; Horita, Z.; Nemoto, M.; Langdon, T.G. The shearing characteristics associated with equal-channel angular pressing. *Mater. Sci. Eng. A* **1998**, *257*, 328–332.
31. Langdon, T.G. Processing of ultrafine-grained materials using severe plastic deformation: Potential for achieving exceptional properties. *Rev. Met.* **2008**, *44*, 556–564.
32. Løken, S.; Solberg, J.K.; Maehlen, J.P.; Denys, R.V.; Lototsky, M.V.; Tarasov, B.P.; Yartys, V.A. Nanostructured Mg-Mm-Ni hydrogen storage alloy: Structure-properties relationship. *J. Alloy. Compd.* **2007**, *446–447*, 114–120.
33. Girard, G. Etude de nouvelles formes de matériaux basés sur le magnésium pour le stockage réversible de grandes quantités d'hydrogène—Effet d'addition d'éléments de transition. Ph.D. Thesis, Joseph Fourier University (Grenoble 1), Grenoble, France, 2009.
34. *Novel Efficient Solid Storage for Hydrogen*, 2011; NESSHY—Publishable Final Activity Report. Available online: http://www.nesshy.net/images/File/Results/NESSHY%20Final%20Publishable%20Activity%20Report.pdf. (accessed on 23 August 2012).
35. Nah, J.J.; Kang, H.G.; Huh, M.Y.; Engler, O. Effect of strain states during cold rolling on the recrystallized grain size in an aluminum alloy. *Scr. Mater.* **2008**, *58*, 500–503.
36. Lee, S.H.; Saito, Y.; Tsuji, N.; Utsunomiya, H.; Sakai, T. Role of shear strain in ultragrain refinement by accumulative roll-bonding (ARB) process. *Scr. Mater.* **2002**, *46*, 281–285.
37. Saito, Y.; Utsunomiya, H.; Tsuji, N.; Sakai, T. Novel ultra-high straining process for bulk materials—Development of the accumulative roll-bonding (ARB) process. *Acta Mater.* **1999**, *47*, 579–583.
38. Tsuji, N.; Saito, Y.; Lee, S.-H.; Minamino, Y. ARB (Accumulative Roll-Bonding) and other new techniques to produce bulk ultrafine grained materials. *Adv. Eng. Mater.* **2003**, *5*, 338–344.
39. Takeichi, N.; Tanaka, K.; Tanaka, H.; Ueda, T.T.; Kamiya, Y.; Tsukahara, M.; Miyamura, H.; Kikuchi, S. The hydrogen storage properties of Mg/Cu and Mg/Pd laminate composites and metallographic structure. *J. Alloy. Compd.* **2007**, *446–447*, 543–548.
40. Mori, R.; Miyamura, H.; Kikuchi, S.; Tanaka, K.; Takeichi, N.; Tanaka, H.; Kuriyama, N.; Ueda, T.T.; Tsukahara, M. Hydrogenation characteristics of Mg based alloy prepared by super lamination technique. *Mater. Sci. Forum* **2007**, *561–565*, 1609–1612.
41. Suganuma, K.; Miyamura, H.; Kikuchi, S.; Takeichi, N.; Tanaka, K.; Tanaka, H.; Kuriyama, N.; Ueda, T.T.; Tsukahara, M. Hydrogen storage properties of Mg-Al alloy prepared by super lamination technique. *Adv. Mater. Res.* **2007**, *26–28*, 857–860.
42. Tanaka, K.; Takeichi, N.; Tanaka, H.; Kuriyama, N.; Ueda, T.T.; Tsukahara, M.; Miyamura, H.; Kikuchi, S. Investigation of micro-structural transition through disproportionation and recombination during hydrogenation and dehydrogenation in Mg/Cu super-laminates. *J. Mater. Sci.* **2008**, *43*, 3812–3816.
43. Wang, J.-Y.; Wu, C.-Y.; Nieh, J.-K.; Lin, H.-C.; Lin, K.M.; Bor, H.-Y. Improving the hydrogen absorption properties of commercial Mg-Zn-Zr alloy. *Int. J. Hydrog. Energy* **2010**, *35*, 1250–1256.